

# Fabrication of a novel microsystem for the electrical characterisation of cell arrays

S. Hediger<sup>\*</sup>, A. Sayah, M.A.M. Gijs

*Institute of Microsystems, Swiss Federal Institute of Technology (EPFL), CH-1015 Lausanne, Switzerland*

Accepted 26 March 1999

## Abstract

We have designed and realised a new type of microsystem for the electrical characterisation of arrays of living cells for biomedical diagnostic purposes. We have used deep plasma etching for the fabrication of microholes and micro-fluidic channels in silicon substrates. After oxidation and electrical contact fabrication, these structured silicon wafers have been anodically bonded with Pyrex wafers. The fabrication is completed by the gluing of micro-patterned polyimide foils on top of the silicon. We have tested the electrical characteristics of our microsystems using NaCl salt solutions of various molarities. We believe that our device will open new perspectives for biochemical sensor applications. © 1999 Elsevier Science S.A. All rights reserved.

*Keywords:* Biological microsystem; Silicon; Micromachining; Living cell; Micro-fluidics

## 1. Introduction

Miniaturised chemical measurements systems, having small-size chemical reaction vessels and sensors for physical and chemical analysis, will have a large impact on the way medical diagnostics will be done in the near future. More particularly, in the field of clinical diagnostics and pharmacology, the use of living cells for fast specific and non-specific chemical sensing is an area of increasing importance [1,2]. A cell is a complex system with appropriate response to a variety of external physical and chemical excitations. Historically, patch clamp and voltage clamp techniques have been used to ‘capture’ and electrically contact single cells and monitor their response to external parameters [3]. With the development of semiconductor manufacturing technology and its derived technologies for the fabrication of three-dimensional microsystems, various micro-tools have become available for the positioning, transport and characterisation of living cells. For example, cells in a liquid environment can be transported now within microchannels by using electro-osmotic flow by applying high voltages across a micro-channel [4,5]. Also microsystems have been proposed for the manipulation and sorting of living cells for application in cytometry [6]. Cell membranes can be micro-perforated using electric

fields, for example in a micro-fabricated cell lysing device [7]. The aim here is to make the cell permeable to a medium so that DNA or RNA can be introduced easily.

Another consequence of the availability of advanced microfabrication techniques is the possibility of increasing parallel analysis on the same chip. For example, silicon nanovial arrays for performing local chemistry in the nl range have been realised [8]. In such device, biochemical reactions with chemical compounds in the nanogram range could be monitored and analysed.

In this paper, we propose a new microsystem, having miniaturised electrical measurement electrodes and integrated microfluidic channels for the electrical characterisation of cells subjected to chemical stimuli. The aim is to facilitate the measurements of cell trans-membrane potentials and chemo-electrical responses. We have realised this microsystem by using photolithography, various etching procedures (among which silicon deep plasma etching), anodic wafer bonding and gluing technologies. We have electrically characterised the system by performing resistance measurements of dilute NaCl solutions of various concentrations.

## 2. Design

Fig. 1a shows a schematic cross-section of the basic cell measurement structure: it consists of a bonded silicon-Pyrex

<sup>\*</sup> Corresponding author. Tel.: +41-21-693-6585; Fax: +41-21-693-5950; E-mail: serge.hediger@epfl.ch

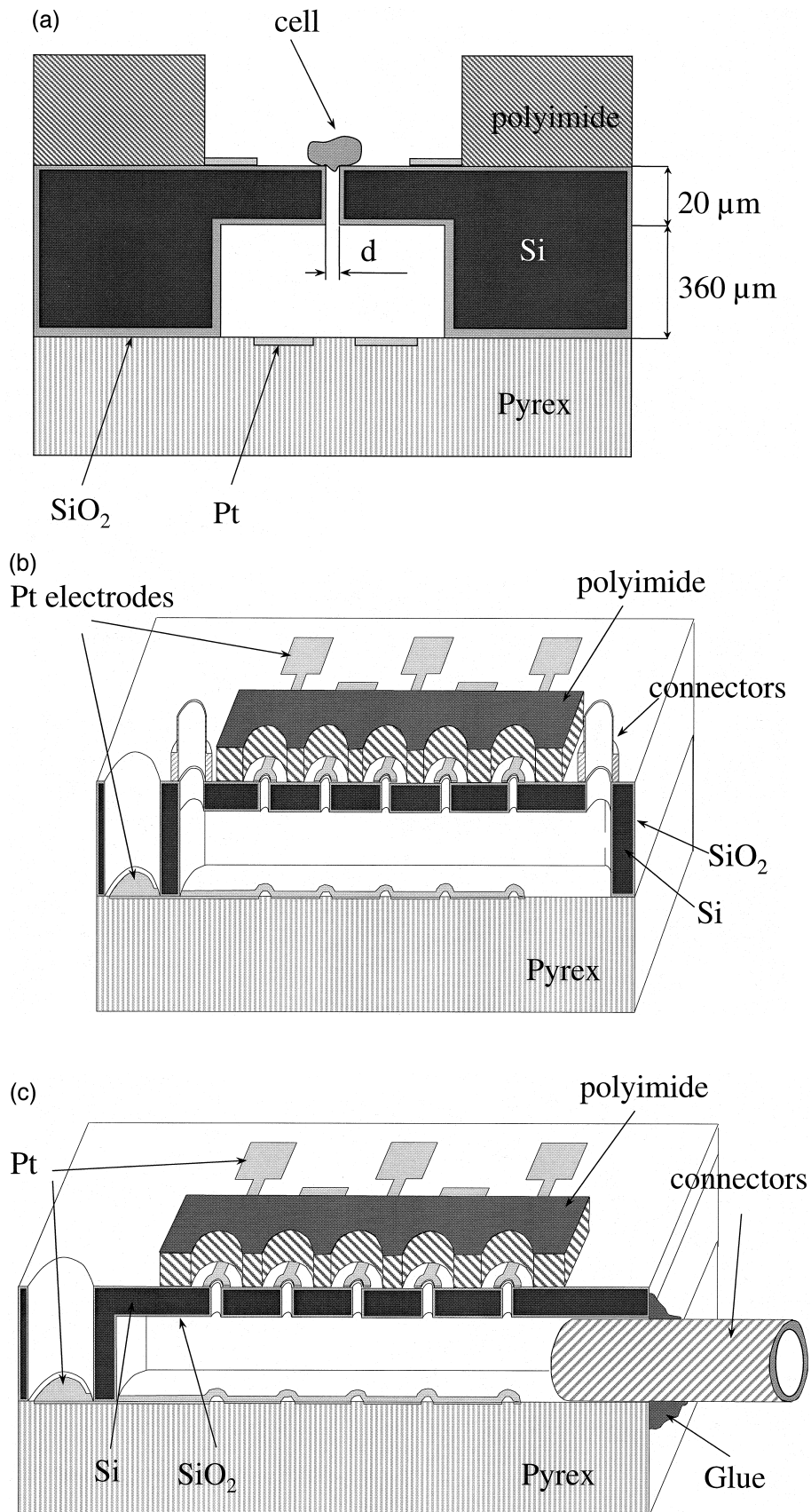


Fig. 1. (a) Schematic cross-section of the basic cell measurement structure. (b) Schematic diagram of a first type of microsystem with top external fluidic connectors. (c) Schematic diagram of a second type of microsystem with side external fluidic connectors.

stack with a microhole of diameter  $d$  patterned in the silicon wafer. Typically,  $d$  should be of the order of  $1\ \mu\text{m}$  or smaller, for firmly fixing a biological cell on top of it (typical cell size  $\sim 10\ \mu\text{m}$ ). We have chosen  $2\ \mu\text{m} < d < 40\ \mu\text{m}$  in our design, whereby the variation in  $d$  is used to check the various critical steps in the fabrication process. Below the microhole, one observes a micro-fluidic channel, formed by etching the silicon wafer from the lower side and bonding it with a Pyrex wafer. Prior to the bonding, the silicon surface is thermally oxidised for electrical insulation purposes. From above, the microhole is situated within a fluid micro-reservoir, defined by micro-patterning a polyimide foil, glued on top of the silicon wafer. Such design leads to a configuration, in which the cell is fixed on top of the microhole and can, at all sides, be surrounded by a biological liquid. For electrical contacting the cell via these conducting liquids, we have provided the structure with concentric electrodes in the top and bottom fluidic reservoir. The basic cell measurement structure of Fig. 1a is repeated to form a five-microhole array, as schematically shown in Fig. 1b,c. Fig. 1b is a first type of structure in which the lower microfluidic channel is accessible from the outside via two external connectors attached on top of the silicon wafer. One also observes one common electrode in the lower micro-fluidic channel for the five microholes. This electrode is accessible from the top through a large hole in the silicon wafer. Fig. 1c shows a schematic diagram of a second type of microsystem, which differs from the first type only by a lateral positioning of the external connectors to the lower micro-fluidic channel. Evidently, such design leads to an improved access to the top of the device, as may be needed for microscopic observations.

### 3. Microfabrication technology

The processing sequence for the realisation of the cell array electrical measurement microsystem is shown in Fig.

2. The fabrication technology involves four lithographic masks and relies on the deep plasma etching of the microholes and the micro-fluidic channel in the silicon, followed by a bonding procedure with a Pyrex glass wafer, on which we have micro-patterned the appropriate electrical contacts. The device is finalised by gluing a microstructured polyimide foil on top of the silicon.

We start with a  $380\ \mu\text{m}$  thick 4 in. (100) silicon wafer with a resistivity of  $0.3\ \Omega\ \text{cm}$ , on which we structure a photoresist mask for the dry etching of the microholes and part of the through-holes (Fig. 2a). We used a  $\text{SF}_6$  deep plasma etch, combined with a  $\text{C}_4\text{F}_8$  sidewall passivation process in a STS reactor, resulting in vertical etch profiles and etch rates of about  $5\ \mu\text{m}/\text{min}$ . The same deep plasma etching process is also used for etching the holes and micro-fluidic channels on the back side of the wafer (Fig. 2b). Next, we perform a thermal oxidation step of the wafer, giving rise to an oxide thickness of about  $0.5\ \mu\text{m}$  on every outer silicon surface, including the microhole and the micro-fluidic channel (Fig. 2c). Subsequently, we structure the top electrical Pt contacts using a photoresist lift-off procedure (see Fig. 2d). The electrical contacts on the Pyrex wafer are also realised using a lift-off process. However, prior to the Pt deposition, we use the lift-off stencil to etch a  $1\ \mu\text{m}$  deep recess (Fig. 2e) in which the Pt contacts will be buried (see Fig. 2f). This procedure gives rise to a flat top Pyrex surface, which leans itself excellently to an anodic bonding assembly with the top silicon wafer (Fig. 2g). In a final step, we glue a mechanically structured  $125\ \mu\text{m}$  thick polyimide foil by heating an intermediate thin film acrylic adhesive layer (Fig. 2h).

### 4. Results and discussion

Fig. 3a,b shows scanning electron microscope (SEM) pictures of two microholes, surrounded by a concentric Pt electrode on top of the silicon wafer. The structure of Fig. 3a has a diameter  $d = 12\ \mu\text{m}$ . The smallest hole structures

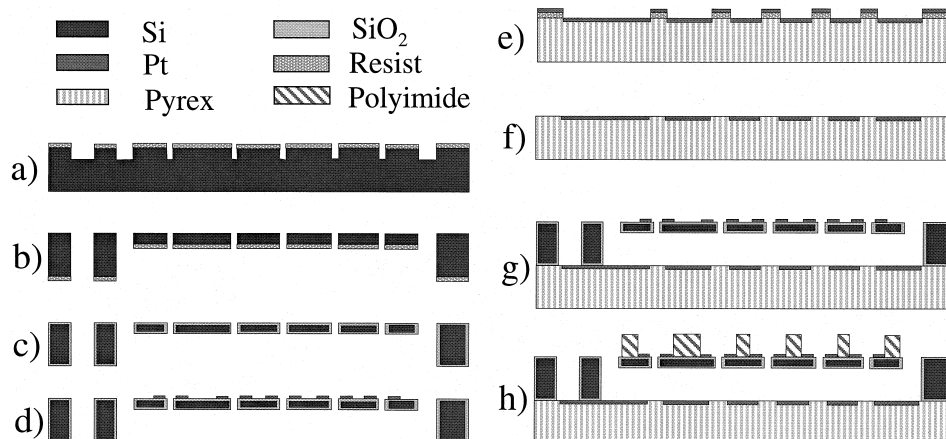


Fig. 2. Schematic cross-section of the processing sequence for the realisation of the cell array electrical measurement microsystem, using four masks.

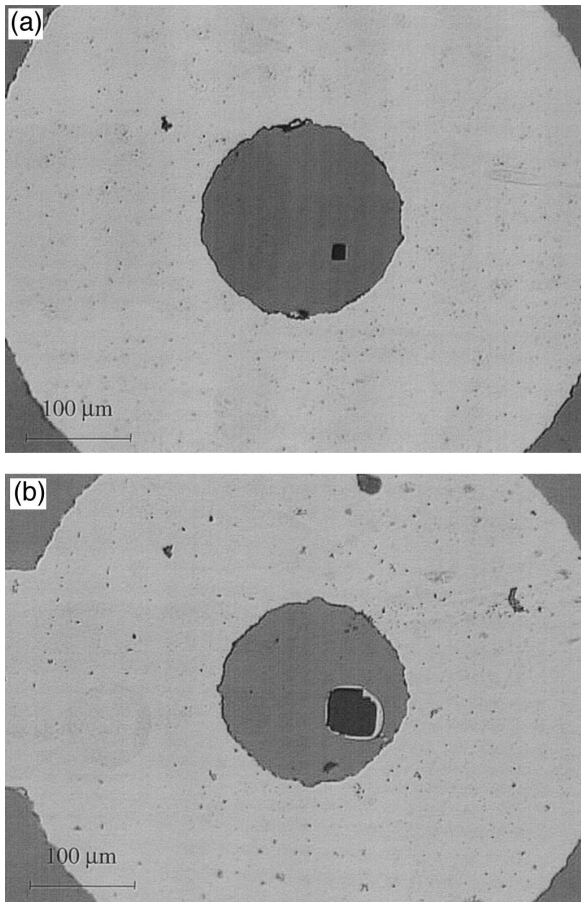


Fig. 3. (a) Optical microscope picture of a microhole of diameter  $d = 12 \mu\text{m}$  surrounded by a concentric Pt electrode. (b) Optical microscope picture of a damaged membrane of a microhole after lift-off procedure, giving rise to a much larger hole.

we realised had inner diameters  $d = 2\text{--}3 \mu\text{m}$  after deep plasma etching; after oxidation of the silicon, the hole diameter can be further decreased with  $0.5\text{--}1 \mu\text{m}$ , due to the volumetric increase of the  $\text{SiO}_2$  with respect to pure silicon. A critical step in microhole realisation is the lift-off procedure of Fig. 2d. Indeed, the subsequent attachment and ultrasonic removal of the photoresist layer risk to damage the membrane in which the microhole is etched. As shown in Fig. 3b, this can give rise to considerably larger microhole diameters, too large for our application; moreover, such membrane breakdown almost certainly leads to an electrical short-circuit, as both the  $\text{SiO}_2$  layer, covering the outer side of the silicon, is removed and the cell will be in direct electrical contact with the top Pt electrode. Fig. 4 shows a detail of the  $0.5 \mu\text{m}$  thick thermal  $\text{SiO}_2$  layer covering the sidewall of the lower micro-fluidic channel. It nicely follows the smooth corner, and thereby prevents electrical leakage through the silicon. The  $\text{SiO}_2$  layer thickness should be chosen appropriately, not too thin to provide electrical insulation and not too thick to disable the anodic bonding process of the silicon

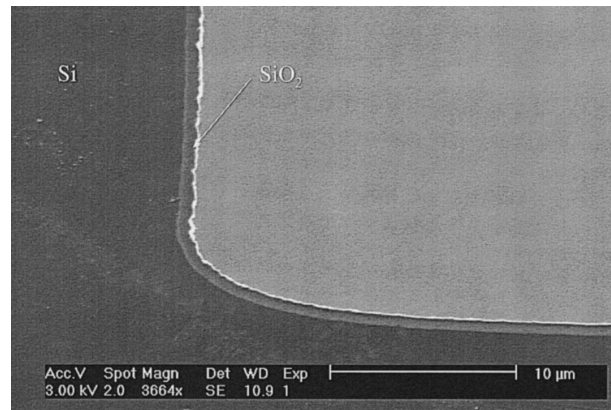


Fig. 4. SEM micrograph of a detail of the  $0.5 \mu\text{m}$  thick thermal  $\text{SiO}_2$  layer covering the sidewall of the lower micro-fluidic channel.

with the lower Pyrex wafer. Fig. 5a is a SEM micrograph, showing a cross-section of the silicon-Pyrex stack at the microhole position ( $d = 40 \mu\text{m}$ ). This picture clearly shows

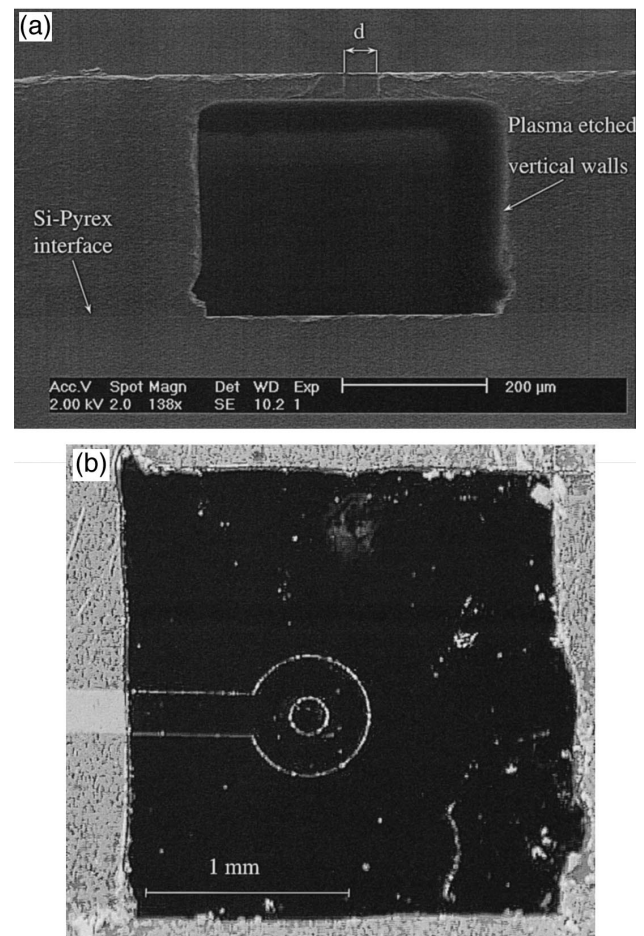


Fig. 5. (a) SEM micrograph of a cross-section of the silicon-Pyrex stack at the microhole position. (b) Optical microscope picture of a top view of a reservoir created by a mechanically structured polyimide layer on top of the silicon. The polyimide thickness in this example is  $25 \mu\text{m}$ .

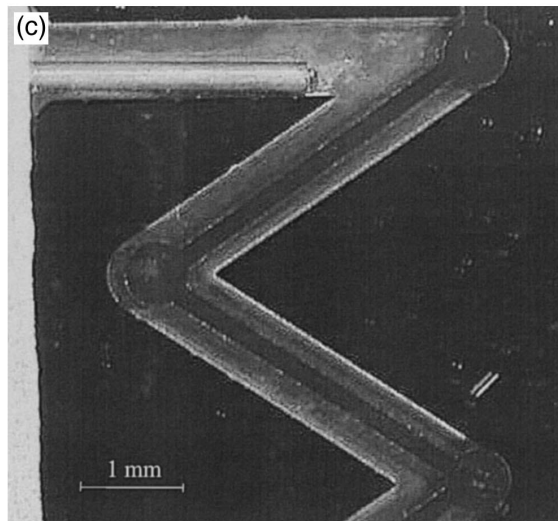
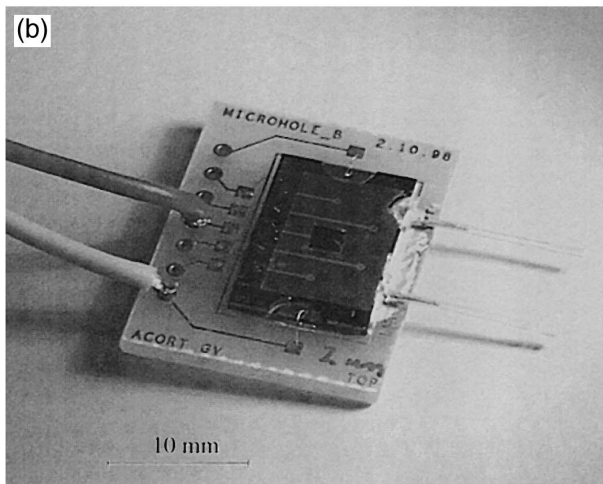
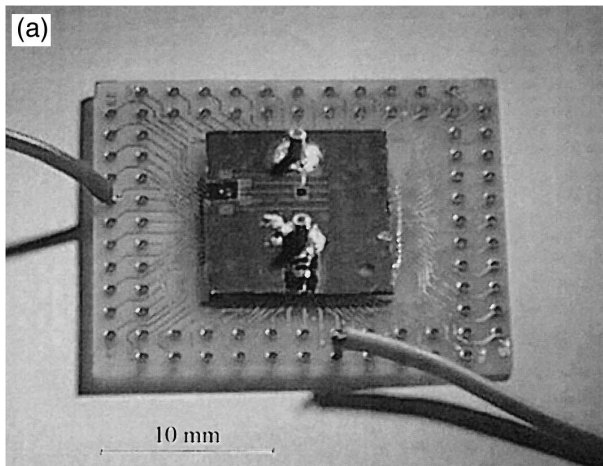


Fig. 6. (a) Photograph of a PCB mounted microsystem for measuring one cell position (one top reservoir), with top micro-fluidic connectors. (b) Photograph of a PCB mounted microsystem for measuring one cell position (one top reservoir), with side micro-fluidic connectors. (c) Optical microscope picture of the bottom side of the second type structure. One observes the lower micro-fluidic channel, the common lower electrode and one of the side micro-fluidic connectors (left).

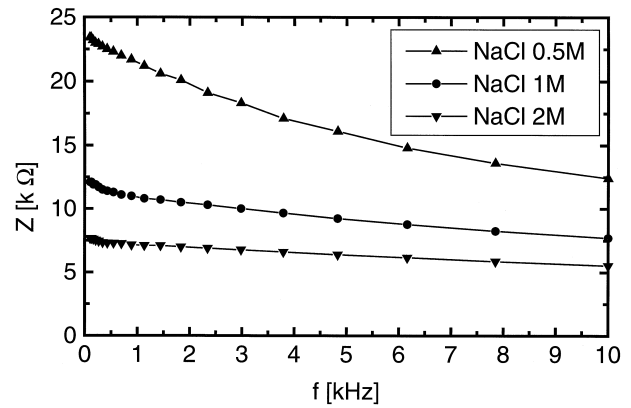


Fig. 7. Impedance versus frequency of a 50  $\mu\text{m}$ -wide microhole measured with three different NaCl salt solutions.

the nearly vertical profiles originating from the plasma etching and the good quality of the silicon-Pyrex bonded interface. Fig. 5b shows a top view of the reservoir created by a mechanically structured polyimide layer on top of the silicon. The polyimide thickness in this example is 25  $\mu\text{m}$  giving a depth of the top micro-fluidic reservoir of 50  $\mu\text{m}$ , taking into account the 25  $\mu\text{m}$  thick gluing foil. One can easily extend this depth range by choosing for an intrinsically thicker foil or for multi-layer polyimide foil configurations. Fig. 6a is a printed circuit board (PCB) mounted microsystem for measuring one cell position (one top reservoir). This structure has the micro-fluidic connectors on top, according to our first design; these connectors are made of steel and are firmly glued using a conductive epoxy paste. One observes that a relatively large surface area is occupied and non-accessible for observation with an optical microscope. This contrasts with the microsystem of Fig. 6b, having the micro-fluidic connectors at the side. Such design obviously gives rise to an optimum use of the wafer surface and allows easy visual control. Fig. 6c is a view of the bottom side of the structure of Fig. 6b. Through a hole in the PCB, one observes the microsystem with a 'meandering' microfluidic channel through the lower Pyrex wafer. This channel geometry was chosen, rather than a straight channel, to optimise the use of the wafer surface.

The basic content of this paper is the design and technology development of a new microsystem, which will be used for biomedical cell diagnostics in the near future. However, after finalisation of the microsystem fabrication and prior to its proper use, we have measured the frequency dependent electrical impedance ( $100 \text{ Hz} < f < 10 \text{ kHz}$ ) of our devices, using a HP4194A Impedance/Gain-Phase analyser. We have prepared NaCl salt solutions of various molarity and, hence, resistivity and injected these fluids within the microholes fluidic reservoirs. Fig. 7 shows the impedance for a 50  $\mu\text{m}$  wide microhole, measured with three different NaCl salt solutions. The resistivities of the 0.5 M, 1 M and 2 M NaCl solutions are 0.44  $\Omega \text{ m}$ ,

0.26  $\Omega$  m and 0.20  $\Omega$  m, respectively. We observe, at low frequency, impedance values of the order 10–30 k $\Omega$ ; with increasing frequency, the impedance drops due to the increasing capacitive coupling in the NaCl water solutions. This was checked independently by measuring the frequency dependent impedance of long plastic tubes, filled with the same NaCl solutions. We can estimate the DC resistance of the fluidic volume of the microhole and connected micro-channel as  $R = \rho[(l_{\text{hole}}/S_{\text{hole}}) + (l_{\text{channel}}/S_{\text{channel}})]$  with  $l_{\text{hole, channel}}$  and  $S_{\text{hole, channel}}$  the length and cross-section of the microhole and microchannel, respectively. For the structure of Fig. 7, we find  $R \approx \rho[\Omega \text{ m}] \times 8.5 \cdot 10^4 [\text{m}^{-1}] = 10\text{--}40 \text{ k}\Omega$  for the various salt solutions, which is close to the AC impedance values we find in our experiments.

## 5. Conclusions

We have designed and realised a new type of microsystem for the electrical characterisation of arrays of living cells for biomedical diagnostic purposes. We have used deep plasma etching for the fabrication of microholes and micro-fluidic channels in silicon substrates. After oxidation and electrical contact fabrication, these structured silicon wafers have been anodically bonded with Pyrex wafers. The fabrication is completed by the gluing of micro-patterned polyimide foils on top of the silicon. After PCB mounting and Al wire bonding, we have tested the electrical characteristics of our microsystems using NaCl salt solutions of various molarities. This allowed us to verify

geometric design parameters and micro-fluidic behaviour. Although more developments are needed, predominantly on the biomedical side, to lead to a fully operational biosensor, we have demonstrated here the feasibility of the microsystem production and initial electrical testing. We believe that our device will open new perspectives for novel and integrated chemical biosensor applications.

## References

- [1] G. Fuhr, Examples of three-dimensional microstructures for handling and investigation of adherently growing cells and submicron particles, *Anal. Methods Instrum.*, Special Issue  $\mu$ TAS '96 (1996) 39–54.
- [2] G. Fuhr, S.G. Shirley, Cell handling and characterisation using micron and submicron electrode arrays, *J. Micromech. Microeng.* 5 (1995) 77–85.
- [3] N.B. Standen, P.T.A. Gray, M.J. Whitaker (Eds.), *Microelectrode Techniques*, The Company of Biologists, Cambridge, 1987.
- [4] D.J. Harrison, P. Li, T. Tang, W. Lee, Manipulation of biological cells and of DNA on-chip, *Anal. Methods Instrum.*, Special Issue  $\mu$ TAS '96 (1996) 147–149.
- [5] P.E. Andersson, P.C.H. Li, R. Smith, R.J. Szarka, D.J. Harrison, Biological cell assays on an electrokinetic microchip, *Proceed. Transducers '97, 1997 Int. Conf. On Solid-State Sens. and Actuat.*, Chicago, 1997, pp. 1311–1314.
- [6] J.G. Blankenstein, L. Scampvia, J. Branebjerg, U.D. Larsen, J. Ruzicka, Flow switch for analyte injection and cell/particle sorting, *Anal. Methods Instrum.*, Special Issue  $\mu$ TAS '96 (1996) 82–84.
- [7] S.W. Lee, H. Yowanto, Y.C. Tai, A micro cell lysis device, *The 11th Int. Workshop on Micro Electro Mechanical Systems MEMS '98*, Heidelberg, Germany, Jan. 25–29, 1998, pp. 443–447.
- [8] J. Roeraarde, M. Stjernström, A. Emmer, E. Litborn, U. Lindberg, Nanochemistry and nanoseparations of biomolecules, *Anal. Methods Instrum.*, Special Issue  $\mu$ TAS '96 (1996) 34–38.